Biointerface Research in Applied Chemistry
Open-Access Journal (ISSN: 2069-5837)

Review
Volume 14, Issue 4 2024, 83
https://doi.org/10.33263/BRIAC144.083

Electrochemical Synthesis of Metal Nanoparticles: A Review

Orest Kuntyi [1], Liliya Bazylyak [2,*], Andriy Kytsya [2], Galyna Zozulya [1], Mariana Shepida [1]

[1] Department of Chemistry and Technology of Inorganic Substances, Lviv Polytechnic National University, 12 Bandery Str., 79013, Lviv, Ukraine; kunty@ukr.net (O.K.); gzozula@ukr.net (G.Z.); maryana_shepida@ukr.net (M.S.);
[2] Department of Physical Chemistry of Fossil Fuels of the Institute of Physical-Organic Chemistry and Coal Chemistry named after L.M. Lytvynenko of the National Academy of Sciences of Ukraine, Lviv 79060, Ukraine; andriy_kytsya@yahoo.com (A.K.); bazylyak.liliya@gmail.com (L.B.)
* Correspondence: bazylyak.liliya@gmail.com (L.B.);

Scopus Author ID 6507438296
Received: 7.06.2023; Accepted: 20.12.2023; Published: 20.07.2024

Abstract: Electrochemical synthesis of metal nanoparticles (MNPs) is a direction of nanoscience and nanotechnology intensively developing in recent decades. This is due to a number of technological advantages of this method, namely, obtaining metal nanoparticles of high purity with the controlled formation of their geometry, the absence of chemical reducing agents, and, accordingly, ensuring the "green" synthesis. This work presents an analysis of the references on the synthesis of metal nanoparticles by electrolysis in aqueous solutions, non-aqueous medium–ionic liquids, and organic aprotic solvents. A modern interpretation of the mechanism of the nucleation and of the formation of MNPs is given. The main factors, particularly the nature of metals, electrolyte composition, electrolysis parameters determining the geometry of nanoparticles, and their size distribution, were analyzed. Attention is focused on the influence of the nature and concentration of surfactants on the formation of nanoparticles and their stabilization. Features of the electrochemical synthesis of metal nanoparticles (silver, gold, platinum, and non-ferrous metals) in aqueous solutions and in the non-aqueous medium are described. The main areas of application of electrochemically synthesized metal nanoparticles are given.

Keywords: metal nanoparticles; electrochemical synthesis; mechanism; aqueous solutions; ionic liquids; organic aprotic solvents; application of metal nanoparticles.

Abbreviations: acac – bis(acetylacetonate); AN - acetonitrile; BDHAC – benzyldimethylhexadecylammonium chloride; BMIm – 1-butyl-3-methylimidazolium; BMP – 1-butyl-1-methylpyrrolidinium; BMP-SAL – 1-butyl-1-methylpyrrolidinium salicylate; BMPTFSA – 1-butyl-1-methylpyrrolidinium bis(trifluoromethylsulfonyl)amide; CHI – chitosan; CTAB – cetyltrimethylammonium bromide; CTAC – cetyltrimethylammonium chloride; DDT – dodecanethiol; DMF – N, N-dimethylformamide; DMSO – dimethylsulfoxide; E0 – standard electrode potential; GC – glassy carbon; icathode – cathode current density; IL – ionic liquids; MMT – sodium montmorillonite; MNCs – metal nanoclusters; MNPs – metal nanoparticles; Na-LS – Na-lauryl sulphate; NaPA – sodium polyacrylate; PANI – polyaniline; PEG – polyethylene glycol; PVA – polyvinyl alcohol; PVP – polyvinylpyrrolidone; RL – rhamnolipid; TBAA – tetrabutylammonium acetate; TBAC – tetrabutylammonium chloride; TBAN – tetrabutylammonium nitrate; TDoAC – tetradodecylammonium chloride; Tf2N- – bis(trifluoromethanesulfonyl)imide; TGA – thioglycolic acid; THF – tetrahydrofuran; TMHATFSA – trimethylhexylammonium bis(trifluoromethylsulfonyl)amid; TPP – triphenylphosphine; TTAB – tetradodecylammonium bromide.

1. Introduction

Today, metal nanoparticles (MNPs), due to their chemical and physical properties as well as to nanoscale effect, have a much wide application in many different areas, in particular in antimicrobial and biomedical ones [1–8]; they can be applied as antimicrobial agents in the agricultural area [9, 10] and in textile industries [10, 11]; at the same time, MNPs are often used for wastewater treatment [10, 12–14], for sensing of ion metals, organic and biomolecules [10, 15, 16] as well in the catalysis [10, 12–14] (Fig. 1).

The functional properties of metal nanoparticles (chemical, antibacterial, catalytic, magnetic, optical, etc.) depend on the shape and the size, as well as on the surface charge and the surface area. Thus, the geometry of MNPs significantly affects their properties, in particular, antimicrobial [17] and catalytic [18] activities. In the tuple, *the methods and conditions of synthesis → geometry → properties → function → field of application*, the first participant is decisive. Therefore, the choice of a method for synthesizing metal nanoparticles, which maximally ensures the controllability of the formation of MNPs according to their geometry, is one of the main priorities of nanomaterials science.

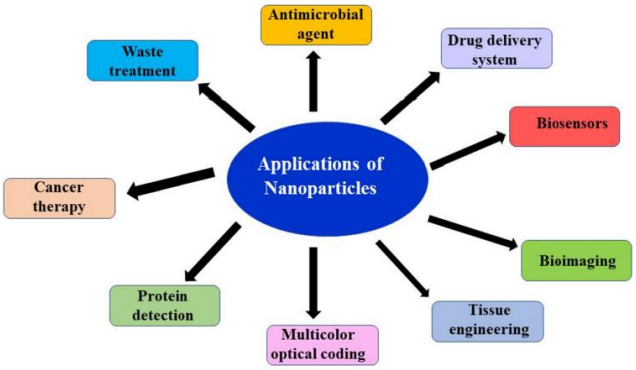

Figure 1. Different branches of the applications of metal nanoparticles (MNPs) [12]. Presented under the terms of the Creative Commons CC BY license.

Methods of the synthesis of MNPs and non-metals, as well as compounds, are divided into physical and chemical groups. Suppose the first methods are implemented without the changes in the degree of oxidation of the metal. In that case, the second group of the methods necessarily includes the redox reactions, regardless of how the nanoparticles are formed – *bottom-up* process or *top-down* process (Fig. 2). In addition to the controlled formation of metal nanoparticles by geometry, the strategy for metal nanoparticle obtaining includes their "*green*" synthesis. The latter includes the use of non-toxic reducing agents and stabilizers of natural origin, which are components of plants [4, 5, 9, 12, 19], bacteria [4, 8, 10, 20–22], algae [4, 20, 23], and fungi [4, 10, 20, 24]. The methods of obtaining MNPs by the electrolysis [25–27], as well as applying the additional physical factors (for example, ultrasonic irradiation [26]), can be attributed to the "green" synthesis due to the exclusion of the use of chemical reducing agents. The main advantage of electrochemical synthesis is obtaining high-purity metal nanoparticles with controlled geometry formation.

The purpose of the work is a comprehensive analysis of the scientific references on the electrochemical synthesis of metal nanoparticles, covering the following: modern interpretation of the mechanism of the nucleation and the growth of MNPs; the dependence of the size and shape of nanoparticles on electrolysis conditions (electrolyte composition and electrolysis parameters); an influence of the nature and the concentration of surfactants on the formation of nanoparticles and their stabilization; the examples of electrochemical synthesis of

nanoparticles of silver, gold, platinum and non-ferrous metals in aqueous solutions and non-aqueous medium (ionic liquids and organic aprotic solvents); areas of MNPs application.

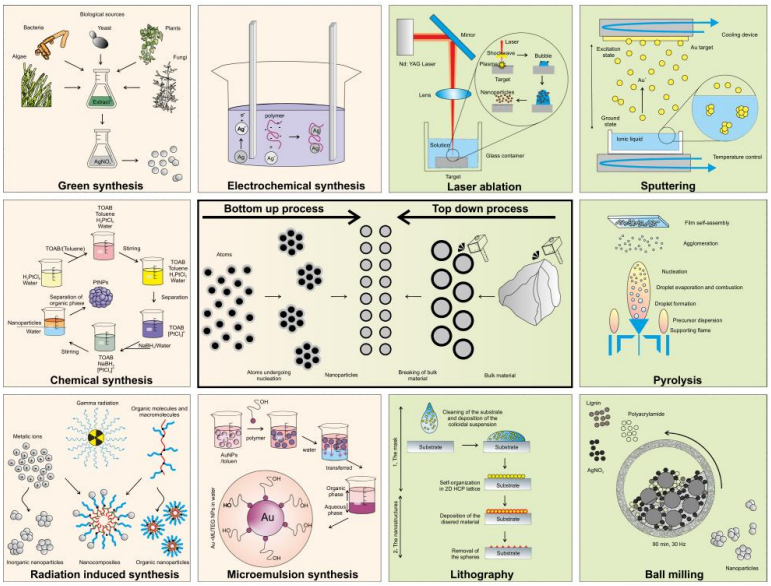

Figure 2. Schematic representation of the *top-down* (images with a green background) and *bottom-up* (images with pale yellow background) approaches of nanoparticle synthesis [19]. Presented under the terms of the Creative Commons CC BY license.

2. Mechanism of Electrochemical Synthesis of MNPs

The electrochemical synthesis of metal nanoparticles in aqueous solutions and non-aqueous media is based on reducing metal ions via reaction (1). However, depending on the conditions of electrolysis, it is possible to proceed with two competing processes: first is the deposition of metal on the cathode surface, and second is the formation of stabilized MNPs in the solution volume.

$$M(+n) + ne^- \longrightarrow M(0) \qquad (1)$$

1. The following main consecutive steps take place during the formation of metal deposits on the cathode surface, namely: *1) transfer of metal ions from the bulk of the electrolyte to the electrode surface by diffusion → 2) reduction to the metal atom via reaction (1) → 3) adsorption on the electrode surface (adatom) → 4) growth of the metal crystal (crystallization)*. The last step, depending on the value of cathode current density (or cathode potential), causes the formation of deposits of various structures. Thus, at law $i_{cathode,}$ the metal coatings are formed; at high ones, the dendrites and even metal powders can be formed.

2. The electrochemical formation of the nanoparticles with the production of colloidal solutions of MNPs has occurred if the crystal growth of the metals is prevented or at least weakened. To implement this, i.e., to prevent the third and fourth of the above-mentioned steps, which occur during the deposition of metals on the cathode surface, the surfactants are introduced into the electrolyte. Electrolysis is carried out in an extreme region of the cathode current density (extremely negative potential region) and at very low concentrations of metal ions. At the same time, a peculiar blocking layer from the cations of surfactants is formed on the cathode surface, which is typically for the environment of ionic liquids [28–32] and organic aprotic solvents [33–35]. In aqueous solutions, the cations of surfactants are also used [36–38], but more often the polar organic molecules are applied [39–44]. Organic radicals included in such cations, for example, 1-hexyl-1-methylpyrrolidinium (HMP^+) and 1-decyl-1-

methylpyrrolidinium (DMP^+) [29], 1-butyl-1-methylpyrrolidinium bis(trifluoromethylsulfonyl)amide (BMPTFSA) [30], tetraalkylammonium [34], create the steric hindrance near the surface of the cathode. In aqueous solutions, for example, the tetradodecylammonium cation [38] also gives hydrophobicity to the blocking layer.

If there is a blocking layer from the cations of surfactants on the cathode surface, then as the authors allow [29], electron transfer is possible by tunneling. The latter also can occur in the presence of adsorbed polar organic solvents. Therefore, there is a probability of reducing the metal ions to atoms (1) on the surface or in the volume of the absorbed layer of the surfactant. The presence of an anionic complex of a reducible metal in the electrolyte is also a restraining factor for the deposition of MNPs on the cathode surface since its negative charge complicates its adsorption. Most often, these are complexes with inorganic ligands – $[AuCl_4]^-$ [45], $[PdCl_4]^{2-}$ [46, 47], $[PdBr_4]^{2-}$ [29], $[PtBr_4]^{2-}$ [48]. In aqueous solutions, even in the presence of surfactants, partial deposition of the metal on the surface of the cathode is observed. The non-stationary current supply is used to avoid, or at least to weaken, such an undesirable process, namely the changing of current polarity [49–51] and cyclic voltammetry [43, 45, 52, 53]. Under such electrolysis, partially deposited metal is dissolved during the anodic period. Effective in terms of preventing metal deposition and, at the same time, the formation of small MNPs with a narrow range of sizes is the use of ultrasound and non-stationary current supply [26].

The mechanism of the binding of metal atoms into nanoclusters and nanoparticles during the electrolysis is practically not covered in the references. Therefore, an analogy is sometimes drawn with the growth mechanism of MNCs and MNPs during chemical synthesis. Thus, the ref. [49] shows the formation of Ag_x^+ "magic" clusters and their growth by analogy with the growth during chemical reduction according to the following scheme [54]:

$$Ag^+ + e \rightarrow Ag \quad (2)$$

$$Ag + Ag \rightarrow Ag_2 \quad (3)$$

$$Ag + Ag^+ \rightarrow Ag_2^+ \quad (4)$$

$$Ag_2 + Ag \rightarrow Ag_3 \quad (5)$$

$$Ag_2^+ + Ag^+ \rightarrow Ag_3^{2+} \quad (6)$$

$$Ag^{a+}{}_x + Ag^+ \rightarrow Ag^{(a+1)+}{}_{x+1} \quad (7)$$

$$Ag^{a+}{}_x + Ag^{b+}{}_y \rightarrow Ag^{(a+b)+}{}_{x+y} \quad (8)$$

The authors [54] showed that at very high rates of reduction, most Ag^+ ions are quickly turned into neutral Ag atoms, which aggregate according to the reactions (3, 5, ...). Under the low rates, the Ag atoms are bonded with Ag^+ ions and charged particles, i. e., via the reactions (4, 6-8). In the case of electrochemical synthesis, the reduction rate is given by the value of current density.

3. The main factors influencing the formation of MNPs by electrolysis in aqueous solutions

The formation of metal nanoparticles during their electrochemical synthesis depends on many factors, including the composition of the electrolyte (the nature of metal ions, surfactants, conductive substances, and their concentrations), the nature of the medium (aqueous or non-aqueous) and electrolysis conditions (values of cathode currents or cathode potentials and forms their supply, electrolyte temperature, ultrasonic field). However, the main one that determines the rate of the reduction of metal ions and, accordingly, the rate of the

nucleation and of the growth of clusters and nanoparticles, that is, the geometry of MNPs, is the $i_{cathode}$ ($E_{cathode}$). This significantly distinguishes electrochemical synthesis from chemical synthesis, which isn't a priority factor influencing the formation of nanoparticles. This section analyzes the parameters that have the most influence on the process of MNPs formation and are the factors of their controlled synthesis based on nanoparticle geometry.

Among them are the most important: current density and current mode; metal ion concentration; surfactant nature and its concentration; temperature; duration of electrolysis; ultrasound; non-aqueous medium. At the same time, the level of coverage of one or the other parameters in scientific publications was also considered.

3.1. Influence of current density and current mode.

Current density is the main electrochemical parameter for regulating the rate of the synthesis of metal nanoparticles and controlling their sizes. The rate of the metal reduction reaction (1) under the galvanostatic mode of electrolysis and, therefore, the rate of the electrochemical synthesis of MNPs depends on the cathode current density. However, in aqueous solutions at certain values, a parallel reaction of hydrogen electroreduction occurs, the proportion of which is increased with the increase of the $i_{cathode}$. In ionic liquids and in organic aprotic solvents, the electrochemical resistance of the solvent is much higher than the electrochemical resistance of water. Therefore, the limiting current density of cathodes in such non-aqueous media can take higher values. The influence of the $i_{cathode}$ on the processes of nanoparticles formation is determined by the energetic character of this electrolysis parameter, taking into account the large difference between the energy of nucleation and the energy of nanoparticles growth. For example, the activation energy (E_A) of AuNPs nucleation equals 92.7·kJ·mol^{-1}, while E_A of their growth is 24.6 [55]. Therefore, the large values of current density contribute to the process of nucleation, and small values to the process of the MNPs growth. It was shown for the first time by Reetz' [33] in the example of the PdNPs formation that an increase of the value $i_{cathode}$ causes to decrease of nanoparticles. For example, at $i_{cathode}$ = 0.15 and 5mA·cm^{-2} the average particle diameter is 4.8, and 1.4 nm, respectively. A similar pattern is observed during the electrochemical synthesis of nanoparticles of other metals and binary systems in aqueous solutions and non-aqueous media (Table 1).

Table 1. An influence of the conditions of electrochemical synthesis on the characteristics of MNPs.

MNPs	$i_{cathode}$, mA·cm^{-2}	Average particle size, nm	medium	Ref.
AgNPs	1.35; 2.85; 4.14 and 6.90	6 ± 0.7; 4.5 ± 0.8; 3.2 ± 0.6 and 1.7 ± 0.4	AN	[49]
AuNPs	1; 2 and 3	53.7; 32.1 and 12.2	aqueous	[38]
	6 and 10	36 and 25	AN:THF=4:1	[56]
PdNPs	50 and 100 mA (rotating electrode)	22.2 and 7.6	aqueous	[46]
	100; 150; 250 and 350	34; 26; 17 and 8	aqueous	[47]
	50; 100 and 150	22 ± 8; 19 ± 7 and 10 ± 4	aqueous	[57]
	1.11; 0.74; 0.37 and 0.19	2.4; 2.9; 3.5 and 3.9	IL	[58]
	0.74 and 0.37	2.4 and 3.2	IL	[59]
	1; 2 and 3	4.10; 3.58 and 3.00	IL	[60]
	0.1; 0.8 and 5.0	4.8; 3.1 and 1.4	AN+THF	[33]
	0.2; 1.0 and 4.0	4.1; 2.5 and 2.0	AN	[34]
	2.16 and 5.41	2.56 and 1.39	THF	[61]
CoNPs	1; 2; 3 and 5	7; 3; 2 and 2	AN	[62]
RhNPs	0.5; 1.5 and 2.5	3.2; 1.8 and 2.5	aqueous	[63]
RhPdNPs	1; 2 and 5	5.2 ± 0.2; 2.0 ± 0.1 and 5.2 ± 0.2	aqueous	[64]

With increasing the values of cathode current density, a “blue shift” in the plasmon peak is also observed, which confirms the tendency to the “shredding” of nanoparticles [65, 66]. In the example of the electrochemical synthesis of AgNPs, it was shown that the increasing of the $i_{cathode}$ from 5 to 50 mA·cm^{-2} causes a shift of λ_{max} on the UV-Vis absorption spectra from 440 to 405 nm, respectively. At the same time, the nature of the curves practically does not change (Fig. 3).

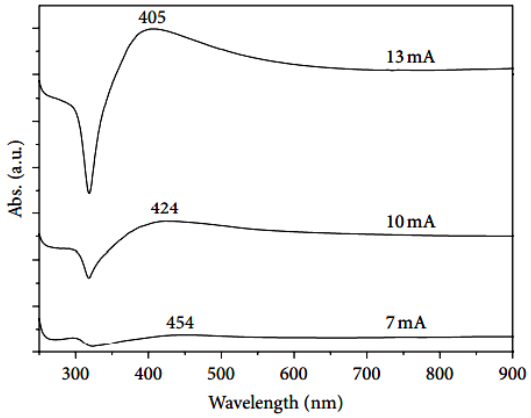

Figure 3. UV-Vis spectra of Ag nanoparticles were obtained by using different current densities during the synthesis process. From the bottom to the top: 7 mA, 10 mA, and 13 mA. In the figure, the plasmon position is indicated for each spectrum [41]. Presented under the terms of the Creative Commons CC BY license.

Sometimes, the current density is used to obtain the shape of the metal nanoparticles. For example, in ref. [67] it was shown that zero-dimensional, spherical, oval shapes and 3D AgNPs can be obtained by sonoelectrochemical synthesis of AgNPs with controlled values of the cathode and the corresponding concentration of surfactants. As it was already mentioned, the electrochemical synthesis of MNPs at E = constant or $i_{cathode}$ = constant, even in the presence of surfactants, leads to the formation of nanoparticles with a wide range of sizes and contributes to their deposition on the surface of the cathode. To prevent such undesirable consequences of stationary electrolysis, the non-stationary current supply to the electrodes is widely practiced, namely the changing polarity between silver electrodes [49, 50, 68–74] and cyclic voltammetry [43, 45, 52, 53].

3.2. Influence of metal ion concentration in solution.

The rate of metal reduction in solutions or on the surface of the cathode is proportional to the concentration of the corresponding ions. Therefore, for the formation of small-sized MNPs, the solutions of M(+n) salts with very low concentrations are used (from 10^{-5} to 10^{-4} mol·L^{-1}) both for chemical [5, 24] and electrochemical [52, 65] synthesis.

The influence of concentration on the size of nanoparticles should be considered, taking into account the type of metal ion, namely solvated or complex one. In the latter case, the stability of the complex plays an important role. After all, the more stable the complex, the smaller the concentration dependence of the size of the nanoparticles. However, for the formation of MNPs of a given geometry, the electrochemical synthesis must be carried out at the constant concentration of the metal ion in the solution, regardless of the type of ion. Effective for this is the use of sacrificial anodes both in aqueous solutions [36, 38, 43, 44, 49–51] and in non-aqueous media - ionic liquids [30, 58–60] and organic aprotic solvents [33, 35, 55, 66, 75–78]. Combining sacrificial anodes and changing polarity between the electrodes or

cyclic voltammetry prevents the anode passivation, ensuring a stable concentration of metal ions during long-term electrolysis.

3.3. Influence of surfactant nature and its concentration.

During the electrochemical synthesis of metal nanoparticles in solutions, the surfactants perform the following functions: 1) blocking of the cathode surface and, accordingly, the prevention of metal deposition on the cathode; 2) the ligands in the complex formation with metal ions; 3) the stabilizers of formed nanoclusters and nanoparticles.

1. The main aspects of blocking the cathode surface by ions or molecules of surfactants and its effect on the formation of MNPs in solutions are considered in Chapter 2. Moreover, the influence of the nature of surfactants on their adsorption was analyzed.

2. In solutions, hydrated and solvated metal ions form complexes with molecules or anions of surfactants. Moreover, they form complexes both with monomeric (Fig. 4, a) and polymeric (Fig. 4, b, c) their forms. The presence of complexes in solutions causes cathodic polarization, which contributes to forming small MNPs.

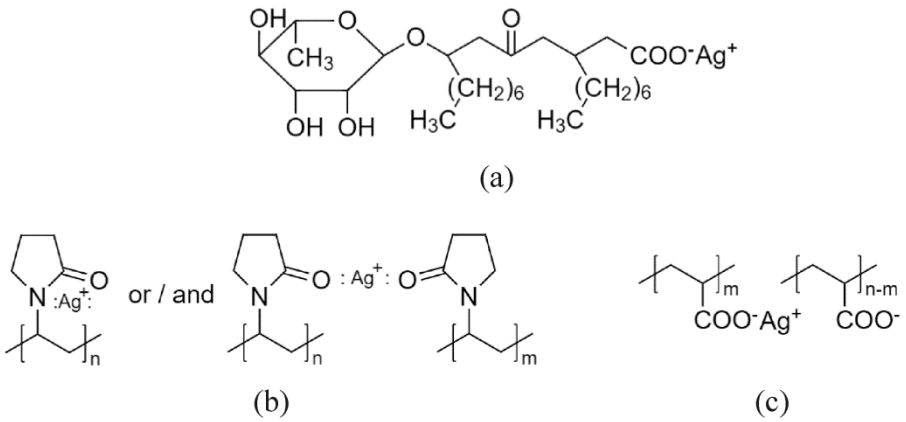

Figure 4. Scheme of complexes Ag(I) with surfactants: **(a)** rhamnolipid; **(b)** polyvinylpyrrolidone; **(c)** polyacrylate.

During the electrolysis with sacrificial anodes, the complexes are formed due to anodic reactions in a solution of monomeric (9) or polymeric (10) surfactants [43, 49].

$$Ag + RL \rightarrow [AgRL]^{+} + e^{-} \quad (9)$$

$$mAg + PA^{n-} \rightarrow [Ag_mPA]^{(n-m)-} + me^{-} \quad (10)$$

3. Stabilization of MNPs occurs due to the adsorption of surfactants on the surface of nanoparticles. The strength of adsorption and, accordingly, the effectiveness of stabilization depends on the nature of surfactants (electrodonating properties and structure) [29, 31, 39, 78, 66] and their concentration in the solution [38, 42, 43, 49, 79–81]. It was shown in ref. [66] the larger the alkyl chains in tetraalkylammonium cations, the smaller the size of AuNPs formed during the electrolysis in an organic aprotic solvent medium. Thus, for the $i_{cathode}$ = 10 mA·cm^{-2} the following dependence "surfactant–∅AuNPs" is observed: TBAC – 7.2 ± 2.9 nm; TOAC – 5.0 ± 1.1 nm; TDoAC – 4.9 ± 1.4 nm. The authors explain this by the higher possibility of forming more compact shells around the nanoparticle if the surfactant has longer (octyl– or dodecyl–) chains compared to short (butyl) chains. A similar regularity is observed with the "blue shift" in the plasmon peak: AuNPs / TBAC – λ_{max} = 525.5 nm; AuNPs / TOAC – 522.4; AuNPs / TDoAC – 519.3. A similar effect of the chain length was detected during the electrochemical synthesis of CuNPs in solutions of tetra-dodecyl ammonium and benzyl-dimethyl-hexadecyl ammonium chlorides (Fig. 5).

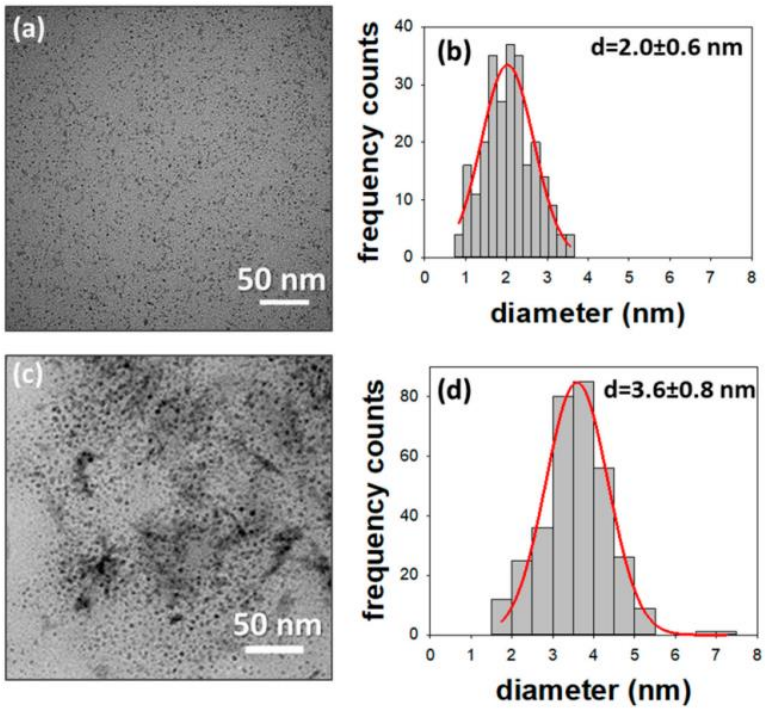

Figure 5. Transmission electron microscopy (TEM) images of the Cu@TDoAC colloid **(a)** and the Cu@BDHAC colloid **(c)**, along with the size distribution histograms **(b, d)**. Sample **(a)** d = 2.0 ± 0.6 nm, n = 250; sample **(c)** d = 3.6 ± 0.8 nm, n = 330 [78]. Presented under the terms of the Creative Commons CC by license.

As the concentration of surfactant increases, the density of the blocking layer on the cathode surface also increases, and the shells around the nanoparticle become more compact. As a result, the size of MNPs is decreased, a typical illustration of which is shown on Fig. 6.

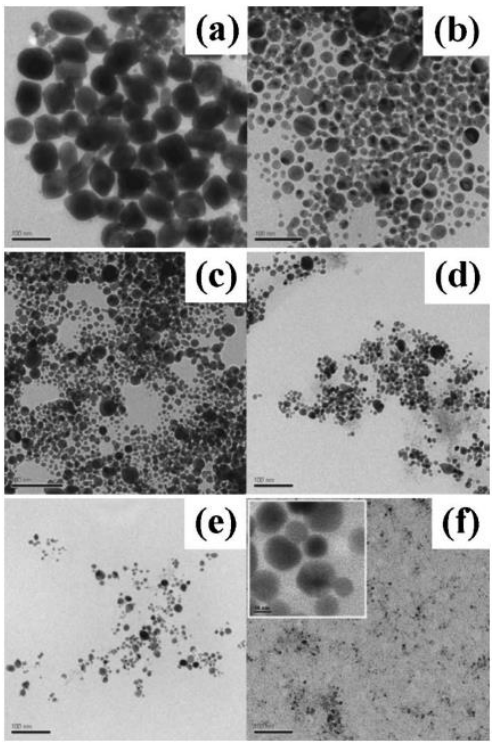

Figure 6. Transmission electron micrographs of gold nanoparticles prepared using different amounts of TTAB surfactant; **(a)** 1; **(b)** 10; **(c)** 30; **(d)** 50; **(e)** 70; **(f)** 90 mg; scale bar represents 100 nm [38]. Presented under the terms of the Creative Commons CC BY license.

The concentration of surfactants can influence the size of electrochemically synthesized MNPs in very wide ranges. Thus, if the content of tetradodecylammonium bromide is increased nine times, then the average size of AuNPs is decreased six times, [38]: 1, 10, 30, 50, 70, and 90 mg·L^{-1} of TTAB – 58.3 ± 12.6, 44.6 ± 18.1, 36.7 ± 19.6, 25.3 ± 11.7, 17.2 ± 10.2, and 10.6 ± 6.5 nm. A similar pattern is observed in the case of the use of polymeric surfactants. Thus, with an increase of the concentration of NaPA from 1 to 4 g·L^{-1}, the average size of AgNPs is decreased from 3.6 ± 1.8 to 1.5 ± 3.9 nm [49], an increase of the concentration of PVP from 2.5 wt % to 5.0 wt % leads to a decrease of AgNPs from about 15 nm to 1~3 nm [79].

3.4. Influence of temperature and duration of electrolysis.

In the chemical methods of the synthesis of metal nanoparticles, the temperature is used as an energy factor since the activation energies of the nucleation process are high [55]. In electrochemical synthesis, the main energy factor is the value of the cathode potential (or $i_{cathode}$), so the electrolysis is mainly carried out at room temperature. An increase in temperature causes the cathodic depolarization to shift the balance of adsorption(desorption of the surfactants on the surface of the cathode on the surface of nanoparticles in the direction of desorption). As a result, the size of nanoparticles is increased [38, 43, 49, 58]. Thus, during the electrochemical synthesis of AuNPs in aqueous solutions containing the surfactants TTAB at temperatures of 25, 40, and 60°C, the average sizes of nanoparticles are 8.3, 34.5, and 53.8 nm, respectively [38]. At the same time, the absorption maxima (λ_{max}) in the UV-Vis spectra are shifted towards the higher values, 521, 530, and 538 nm. Sometimes, the electrochemical synthesis is carried out at temperatures above 80°C (high-temperature electrochemical synthesis) [82–84]. The sizes of electrochemically synthesized metal nanoparticles depend on the ratio of the rate of formation of nuclei to the rate of their growth. This ratio depends on many factors, primarily on the following: type of metal ion (simple or complex) and its concentration, value of current density, nature and concentration of surfactants, and temperature. Accordingly, the influence of the duration of electrolysis on the growth of particles must be considered in the aggregate and interdependence of the specified factors. This can explain the small number of systematic studies concerning the dependence on "*the duration–MNPs size*" [60, 72]. Therefore, one can only consider the growth trend of nanoparticles over time. For example, during the electrochemical synthesis of AgNPs for 2, 5, and 10 min, the sizes are 14.1 ± 0.4, 15.8 ± 0.5 and 20.6 ± 0.5 nm, respectively [72].

4. Synthesis of MNPs in solutions by electrolysis in aqueous solutions

The electrochemical method is the most often presented in the scientific references for synthesizing aqueous solutions for the following metal nanoparticles: AgNPs, AuNPs, PdNPs, and PtNPs. Taking into account the differences in properties and applications, it is appropriate to analyze separately the features of their production.

4.1. Electrochemical synthesis of AgNPs.

Today, silver nanoparticles are the most studied and produced among all metal nanoparticles. This is due to their wide range of functional properties and high compliance with the price–performance criterion [5, 70, 85–87]. Therefore, in the last decade, there has been a trend of increasing interest in the synthesis, research, and new fields of the AgNPs application (Fig. 7). Moreover, the most popular publication was concerned with chemical synthesis, which

also includes the syntheses by electrolysis (table 2). Electrochemical synthesis enables the controlled formation of AgNPs with sizes from 1 to 30 nm, which makes it possible to use them in many fields, namely in medicine [42, 65, 72, 79, 92], pharmacy [50, 92], as the sensors [52, 94], in catalysis [80], etc.

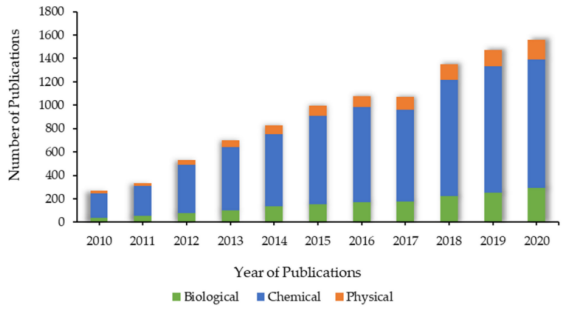

Figure 6. Annual numbers of publications relating to the search terms "Silver nanoparticles" and "Biological/Chemical/Physical" in the Scopus publication database between 2010 and 2020 (English language only) [86]. Presented under the terms of the Creative Commons CC BY license.

As can be seen from Table 2, the majority of AgNPs syntheses are based on the use of sacrificial anodes, which is based on the good anodic solubility of silver in solutions of polymeric [49, 79, 90, 92, 96] and monomeric surfactants [43, 91]. Surfactants are mostly synthetic organic substances, namely PVP [39, 79, 80, 88, 95, 96], PVA [42, 70], PEG [41], NaPA [49, 90], CHI [70, 72, 92]. In recent years, special attention has been paid to the surfactants of natural origin RL [43] and green tea extract [50]. Sometimes, the electrochemical synthesis of AgNPs is carried out without the surfactants [68, 69, 71, 84, 89]. Effective for the controlled synthesis of AgNPs in terms of size, as well as in the technological aspect, is the use of the changing of polarity between silver electrodes using the potentiostatic method [49, 50, 68, 69, 71, 89]. In the last decade, there has been an interest in the research of hybrid methods of synthesizing stabilized AgNPs by electrolysis, particularly by sonoelectrochemical one [26, 98, 99]. Such a method is characterized by the possibility of obtaining the nanoparticles of several nanometers with a narrow range of sizes, as well as by the high speed of the process. The method of galvanic replacement in ultrasound is promising from a technological point of view and as a "green" synthesis [26, 100, 101].

4.2. Electrochemical synthesis of AuNPs.

Gold nanoparticles, due to their high chemical resistance, are biocompatible; therefore, they are attractive in biomedical applications, primarily in cancer therapy, as well as in diagnostics, imaging, and drug delivery [102–104]. AuNPs also exhibit high catalytic properties [105, 106].

Given the great interest in the use of gold nanoparticles in medicine, much attention is paid to their "green" synthesis. Among them, the most studied are syntheses, in which the organic substances of natural origin perform the function of reducing agents and surfactants [102, 104]. Promising "green" synthesis is electrochemical one, which is characterized by wide possibilities of controlled formation of AuNPs by geometry [37, 38, 45, 105-109]. The methods of electrochemical synthesis of AuNPs (Table 3) are not fundamentally differed from the methods of electrochemical synthesis of AgNPs (Table 2). Thus, for the stabilization, similar surfactants are used as well as the electrolysis modes (current density values, current supply methods); the temperature conditions are also insignificantly different. Sacrificial anodes are not used often since gold is anodically stable in many electrolytes.

Table 2. Conditions of AgNPs synthesis by electrolysis in aqueous solutions and their characteristics.

Precursor of metal	Stabilizer	Anode	Parameters of electrolysis	Max. abs. peak (λ_{max}), nm	Particle shape and size (nm)	Applied	Ref.
$AgNO_3$	PEG	platinum rod	2.0; 2.9 and 3.7 mA·cm^{-2}	425	spherical, $\varnothing_{average}$ = 30	–	[41]
$AgNO_3$	PVP, Na-LS	silver plates	1.7– 3.3 mA·cm^{-2}	420	10–55	–	[88]
sacrificial anode	without stabilizer	silver plates	U = 20 V in changing polarity between silver electrodes every 30–300 s. 20–95 °C.	–	spherical, ∅ = 7.3±3.1	–	[89]
$AgNO_3$	CHI	–	U = 5 V, τ = 2; 5; 10 min	~410	14±0.4 (2 min); 15.8±0.5 (5); 20.6±0.5 (10)	antibacterial hydrogel for implants	[72]
sacrificial anode	PVP	silver flakes	1–2 mA·cm^{-2}	~420	spherical about 1~3	in medicines, water treatment	[79]
$AgNO_3$	alginate	platinum plates	5–50 mA·cm^{-2}	405–440	spherical, ∅ = 10–30	antibacterial activity against *Staphylococcus aureus*	[65]
$AgNO_3$	PVP	platinum rod	1 mA·cm^{-2}	420	<35	for tin coating	[39]
sacrificial anode	NaPA	silver plate	E = 0.15 V, t = 20–50 °C	–	spherical, ∅ = 7–10	–	[90]
sacrificial anode	citrate	silver electrode	U = 12 V	~416 nm	spherical, ∅ = 19.7±4.3	antibacterial effectiveness	[91]
sacrificial anode	CHI	silver plate	E = 2 V	420	2–16	in biomedicine and pharmacy	[92]
sacrificial anode	without stabilizer	silver electrode	U = 5–50 V. t = 25–100 °C	around 420	1–10	–	[84]
$AgNO_3$	PVA	platinum plates	25 mA·cm^{-2}	~400, ~650	∅ = 15±9	in biomedicine	[42]
sacrificial anode	MMT	silver plate	U = 5, 10, 15, and 20 V	412	spherical, ∅ = 4.2–25	in antibacterial industry	[93]
sacrificial anode	without stabilizer	silver plates	U = 200 V in changing polarity between silver electrodes (0.5 Hz). 80 °C	399	spherical, ∅ = 1.4–3.7	for the antibiotic burden of patients	[68,69]
$AgNO_3$	PVA and CHI	platinum plate	U = 90 V	396; 407	spherical, ∅ ≈ 10	Ag/PVA/CHI hydrogels in biomedicine	[70]
sacrificial anode	NaPA	silver plate	U = 6 V and frequency of changing of current polarity equals to 1 Hz. 40–60 °C	490–530 (blue line)	spherical, ∅ = 1.5–4.1	–	[49]
$AgNO_3$	PVP	platinum plate	E = −0.10…−6.0 V	~400	spherical, $\varnothing_{average}$ = 30	catalytic activity for the reduction of 4-nitrophenol	[80]
sacrificial anode	RL	silver plate	cyclic voltammetry, E = 1…-1.5 V. 40–60 °C	420–440	spherical, ∅ = 2–20	antimicrobial activity against the bacterial phytopathogens	[43]
sacrificial anode	*Camellia sinensis*	silver plate	U = 4–14 V	437; 443	spherical, $\varnothing_{average}$ = 34	in high-sensitive electrochemical chemosensors	[94]
$AgNO_3$	PVP	boron-doped diamond	E = -1.0 V	~405	$\varnothing_{average}$ = 10	–	[95]
sacrificial anode	without stabilizer	silver plate	U = 200 V in changing polarity between silver electrodes (0.5 Hz). 80 °C	–	$\varnothing_{average}$ = 3	in chemical and biological fields	[71]
sacrificial anode	PVP	silver rods	U = 10 V 60 °C. 60, 80 and 100 mL·h^{-1} flow electrolyte velocity of was used	~420	18.5±4.1; 9.4±1.5; 3.0±0.6 (60, 80 and 100 mL·h^{-1})	–	[96]

Precursor of metal	Stabilizer	Anode	Parameters of electrolysis	Max. abs. peak (λ_{max}), nm	Particle shape and size (nm)	Applied	Ref.
$AgNO_3$	–	platinum wire	E from 0.0 to -0.6 at a scan rate of 100 $mV \cdot s^{-1}$	470	spherical $\varnothing_{average}$ = 8, 20, and 50 at 10, 20, and 30 mM $AgNO_3$	as SERS substrates for Tobramycin detection	[52]
sacrificial anode	green tea extract	silver wires electrodes	U = 10 V, changing polarity of the anode and cathode was varied every 1 min	420	spherical, ∅ = 16.82±4.36	antioxidant in the pharmacy	[50]

Table 3. Conditions of AuNPs synthesis by electrolysis in aqueous solutions and their characteristics.

Precursor of metal	Stabilizer	Anode	Parameters of electrolysis	Max. abs. peak (λ_{max}), nm	particle shape and size (nm)	Ref.
sacrificial anode	TTAB	gold plate	1; 2 and 3 $mA \cdot cm^{-2}$. 25, 40, and 60 °C	522–540	spherical, ∅ = 8.3–58.3	[38]
$H[AuCl_4]$	PVP	platinum plate	cyclic voltammetry (CV) scanning from +0.40 to +0.95 V and back to +0.25 V	570	clusters <2	[45]
[HOOC-4-$C_6H_4N{\equiv}N$]$AuCl_4$	PANI	graphite	E = 0.2, 0.6 and 1.0 V	540	Au−COOH NPs,	[107]
$H[AuCl_4]$	without stabilizer	platinum wires	electroformation of AuNPs in nanoliter droplet reactors	553; 540–526	30–100	[110]
sacrificial anode	PVP	gold wire	alternating voltage (5 V) at 60 Hz is applied to the two Au electrodes	543	nanoicosahedra, 14±3	[51]
sacrificial anode	PVP	gold plate	–	521	<500	[108]
	CTAB	gold plate	U = 1.1, 2.0, 3.0 V	520	spherical, ∅ = 5–70	[37]
$H[AuCl_4]$	PVP	platinum sheet	100 mA	~540	spherical, $\varnothing_{average}$ = 42.4	[40]
$H[AuCl_4]$	PVP	platinum plate	100 mA	~540	spherical AuNPs and plate-like nanoprisms	[111]
$K[AuCl_4]$	–	gold wire	cyclic voltammetry	–	spherical or cubic AuNPs, 20–400	[53]
sacrificial anode	decanethiol	gold wire	electrochemical dissolution of the gold wire electrode at 0.1, 0.3, and 0.5 $A \cdot cm^{-2}$	522	1–3	[44]
$H[AuCl_4]$	PVP	glassy carbon	E = -1.0 V	–	1–10 (average 5)	[109]

4.3. Electrochemical synthesis of nanoparticles of platinum and nonnoble metals in aqueous solutions.

The electrochemical method makes it possible to synthesize metal nanoparticles with high purity and to control their geometry and size distribution [25–27]. This is especially important for the application of MNPs in medicine, catalysis, and sensors. Therefore, almost all metals that can be cathodically reduced in aqueous solutions are studied using electrochemical synthesis in order to obtain the nanoparticles. However, besides the AgNPs (Table 2) and AuNPs (Table 3), the most studied are the nanoparticles of platinum metals (Table 4). This is due to the high chemical activity of metals (M), for which the values of the standard electrode potentials are negative ($E^0 < 0$). Therefore, the stabilization of nanoparticles of such metals is a problem. The stabilization of nanoparticles of those metals for which $E^0 > 0$, such as CuNPs, is sometimes also problematic. In addition, their synthesis must be carried out in an inert medium.

5. Electrochemical synthesis of MNPs in non-aqueous medium

In the last decade, intensive research has been conducted on the chemistry and electrochemistry of metal nanoparticles in non-aqueous media, especially in ionic liquids [28, 114–116] and organic aprotic solvents [117]. This is due to their advantages compared to aqueous solutions, which are especially evidenced during the electrochemical synthesis.

Among them, first of all, there are the following: chemical indifference to nanoparticles, lack of hydrolysis, formation of stable solvates with metal ions, and high electrochemical stability.

Chemical indifference makes it possible to synthesize the MNPs for which the value of the standard metal electrode potential is negative, e.g., SmNPs ($Sm^{3+} + 3e = Sm$, $E^0 = –2.41$ V), FeNPs ($Fe^{2+} + 2e = Fe$, $E^0 = –0.441$ V), CoNPs ($Co^{2+} + 2e = Co$, $E^0 = –0.227$ V) etc. The absence of hydrolysis in a non-aqueous medium, unlike aqueous solutions, simplifies the composition of the electrolyte, as it does not require buffer applications (additives) and reduces the pH factor. The formation of solvates of metal ions, for example, with high-donor organic aprotic solvents, promotes the cathodic polarization and, accordingly, the formation of small nanoparticles. High electrochemical stability makes it possible to carry out the reduction of metal ions at the potentials up to –3 V (Table 5) without side cathodic reactions.

Ionic liquids, as stated in ref. [115], are effective stabilizers of metal nanoparticles and, at the same time, is a medium for catalytic reactions with the participation of MNPs. For the synthesis of nanoparticles in ionic liquids, only the salts of the reducible metal are introduced or a sacrificial anode is used, which simplifies the electrolysis process. In the medium of organic aprotic solvents, a sacrificial anode is mainly used (Table 5).

Table 4. Conditions of MNPs synthesis by electrolysis in aqueous solutions and their characteristics.

MNPs	Precursor of metals	Stabilizer	Electrodes	Parameters of electrolysis	particle shape and size (nm)	Applied	Ref.
PdNPs	$H_2[PdCl_4]$	PVP-8000	rotating Pt cathode, Pt plate anode	E = -0.33 V; 25 and 50 $mA \cdot cm^{-2}$	spherical, 22±4.8 and 7.6±2.2	catalytic activity toward the electrooxidation of methanol	[46]
	$PdCl_2$	CTAC	GC cathode and Pt wire anode	E = -0.9 V	spherical, 5±3	–	[112]
	$H_2[PdCl_4]$	PVP	GC cathode and Pt wire anode	100–350 $mA \cdot cm^{-2}$	spherical, 8–30	high catalytic activity in Suzuki and Heck reactions	[47]
			Pt disc cathode, Pt sheet anode	50; 100; 150 $mA \cdot cm^{-2}$	22±8; 19±7; 10±4	highly efficient catalytic activity on Suzuki–Miyaura coupling reaction efficient catalytic activity in nitroaromatic hydrogenation reaction	[57] [113]
	sacrificial anode		Pd wires as cathode and anode	an alternating voltage of 4 V and 60 Hz	spherical, 1-7	–	[73]
PtNPs	sacrificial anode	PVP	Pt wires as cathode and anode	an alternating voltage of 4 V and 60 Hz	dendrite-like NPs, which consist of several branches ~5	in sensitive enzyme-free biosensor	[74]
RhNPs	$RhCl_3$	TPAB	GC as cathode and Pt wires as anode	-2.5; -1.5; -0.5 $mA \cdot cm^{-2}$	$\varnothing_{average}$ = 2.5; 1.8; 3.2	electrocatalytic activity toward the electrooxidation of methanol	[63]
CuNCs	sacrificial anode	TBAN	Pt sheet cathode and Cu sheet anode	25 $mA \cdot cm^{-2}$	0.61±0.13	in biosensors and biomedicine	[36]
SnNCs	sacrificial anode	PVP	Pt wires as cathode and Sn wires as anode	4.0 V	spherical, ∅ =19±4	in battery	[74]
FeNPs	sacrificial anode	PVA	Pt plate cathode and Fe plate anode	potentiostatic mode at E = 2 V during 8, 24 and 60 h		antibacterial activity against Gram-positive Staphylococcus aureus (S.aureus) and Gram-negative Escherichia coli (E.coli) bacteria	[81]
Pt-PdNCs	sacrificial anode	PVP	Pt plate cathode and Pt–Pd (50:50) wires anode	5.0 V	popcornlike nanoparticles ~40, aggregates of smaller NCrs	–	[74]
Rh-PdNPs	$RhCl_3$ and $PdBr_2$	TPAB	platinum wire cathode and anode	5; 2 and 1 $mA \cdot cm^{-2}$	$\varnothing_{average}$ = 1.9±0.1; 2.0±0.1 and 5.2±0.2	–	[64]

Table 5. Conditions of MNPs synthesis by electrolysis in non-aqueous solutions and their characteristics.

MNPs	Precursor of metal	medium	Electrode	Parameters of electrolysis	particle shape and size (nm)	Ref.
medium of ionic liquid						
AgNPs	$AgNO_3$ and PVP	$[BMIm][BF_4]$	platinum sheets as cathode and anode	100 $mA \cdot cm^{-2}$	spherical shape (~10) and anisotropic hexagons (40–200)	[118]
	sacrificial anode	BMPBr		E = -1.6 V	10-25	[119]

MNPs	Precursor of metal	medium	Electrode	Parameters of electrolysis	particle shape and size (nm)	Ref.
		BMPTFSA	GC as cathode, Ag wire as anode	E = -2.5 V	11±4 nm	[30]
PdNPs	sacrificial anode	Morpholinium Ionic Liquid	Pd foil as anode and Pt foil as cathode	1.11; 0.74; 0.37 and 0.19 mA·cm^{-2}.	$\varnothing_{average}$ = 2.4; 2.9; 3.5 and 3.9	[58]
		[BMIm][BF_4] in AN	palladium foil as cathode and anode	0.74 and 0.37 mA·cm^{-2}	$\varnothing_{average}$ = 2.4 and 3.2	[59]
		[HEMMor][BF_4]		1, 2, and 3 mA·cm^{-2}	4.10, 3.58 and 3.00	[60]
	$[PdBr_4]^{2-}$	bromides of dialkylpyrrolidinium	GC as a working, Pt wire as a counter electrode	E = -2.6 V	from 2.9 to 3.2	[29]
	$PdCl_2$	RTIL BMP-SAL	Pt gauze electrode	E = -1.4 V at 70 °C	<10	[82]
PtNPs	$[PtBr_4]^{2-}$	BMPTFSA	GC	E = -2.6 V	2-3	[48]
	$Pt(acac)_2$	TMHATFSA	GC as a working electrode, Pt wire–counter	E = -1.7 and -2.5 V. 130 °C	3.5±0.7 (-1.7 V); 1.5±0.4 (-2.5 V)	[83]
				E = -1.8 and -2.5 V. 50 °C	2.1±0.8, 2.8±0.8 and 3.0±0.8 at E = -1.8 V	[31]
CoNPs	$[Co(PrIm)_6][Tf_2N]_2$	[BMP][Tf_2N]	Pt covered silicon wafers as working electrode, cobalt plate as anode	E = -3.0 V	<10	[120]
	$Co(TFSA)_2$ and sacrificial anode	BMPTFSA	Pt mesh cathode and Co anode	E = -2.0 V	∅ = 2–10	[121]
NiNPs FeNPs	$Ni(TFSA)_2$ $Fe(TFSA)_2$	BMPTFSA	platinum disk as cathode and platinum wire as anode	E = -2.6 V	∅ = 1.9–3.2 $\varnothing_{average}$ = 4.6	[122]
NiNPs	$Ni(TFSA)_2$	BMPTFSA	GC as cathode, nickel wire as anode	20 μA·cm^{-2}; 25; 100 °C	$\varnothing_{average}$ = 5	[123]
NiNPs	$Ni(HeIm)_6][Tf_2N]_2$ $[Ni(DoIm)_6][Tf_2N]_2$	Tf_2N^-	Pt covered silicon wafers as working electrodes	1 A·dm^{-2}	$\varnothing_{average}$ = 5.4 agglomerates, $\varnothing_{average}$ = 60	[32]
CdNPs	$Cd(TFSA)_2$	BMPTFSA	GC	E = -2.6 V	5–10	[124]
SmCoNPs	$Co(TFSA)_2$ and $Sm(TFSA)_3$	BMPTFSA	GC as cathode, Co wire as anode	E = -1.6 V	aggregates of $SmCo_7$NPs with nanoparticles size <10	[125]
medium of organic aprotic solvents						
AgNPs	sacrificial anode	AN + TBAA	Ag sheet as anode and Pt sheet as cathode	1.35; 2.85; 4.14 and 6.90 mA·cm^{-2}	6±0.7; 4.5±0.8; 3.2±0.6 and 1.7±0.4	[35]
	-	DDT and TBA as surfactants in AN	-	10 mA·cm^{-2}	Ag_5 and Ag_6 clusters	[126]
	sacrificial anode	TGA in DMF	silver rods as cathode and anode	10 mA·cm^{-2}	5–10 in TGA in DMF (absorption peak ~420 nm) and 45 in pure DMF	[75]
	sacrificial anode	DMSO	silver rods as cathode and anode	U = 100 V (200-260 mA·cm^{-2}) at 28±0.2 °C	(absorption peak 425±5 nm)	[76]
AuNPs	sacrificial anode	THF:AN, ratio 3:1 + NR_4Cl (R = C_4, C_8, C_{12})	gold anode and platinum cathode	0.14–4.12 mA·cm^{-2}	4–8	[66]
		AN: THF, ratio 4:1 + tetra alkyl ammonium salt (TEAB, TPAB, TBAB, or TOAB)		6 and 10 mA·cm^{-2}	8.1–10.9	[55]

MNPs	Precursor of metal	medium	Electrode	Parameters of electrolysis	particle shape and size (nm)	Ref.
PdNPs	sacrificial anode	AN: THF, ratio 4:1	palladium anode and a platinum cathode	0.1; 0.8 and 5.0 mA·cm^{-2}	$\varnothing_{average}$ = 4.8; 3.1 and 1.4	[33]
		[R_4N]Br в AN (THF)		0.2–4.0 mA·cm^{-2}	$\varnothing$ = 2.0–4.0	[34]
PdNPs NiNPs PdPtNPs	-	[R_4N]Br в AN (THF)	nickel or palladium anode and platinum cathode	2.1–5.4 mA·cm^{-2}	$\varnothing$ = 1.2–5.0	[61]
CoNPs	sacrificial anode	TOAB in THF	cobalt anode and cobalt cathode	-	$\varnothing_{average}$ = 1.9	[77]
		TBAN in AN + oleic acid and TPP as surfactants	cobalt anode and platinum cathode	1–5 mA·cm^{-2}	2–7	[62]
CuNPs	sacrificial anode	TDoAC or BDHAC in $CHCl_3$ + THF	copper anode and platinum cathode	E = 1.5 V	$\varnothing$ = 2±0.6 (Cu@TDoAC); $\varnothing$ = 3.6±0.8 (Cu@BDHAC)	[78]

6. Conclusions

The electrochemical method provides a controlled synthesis of metal nanoparticles with specified nanoparticle geometry and size distribution as well as high purity of MNPs. The mechanism of formation of metal nanoparticles in aqueous solutions is based on the formation of a blocking layer of molecules or ions of surfactant on the cathode surface. With increased current density and at low concentrations of metal ions in such a layer, the reducing of the ions to the atoms take place with the subsequent formation and stabilization of the nanoclusters and their transition into the volume of the solution. Therefore, the surfactants prevent to the nucleation and to the growth of metal deposits on the cathode.

The main factors affecting the size of metal nanoparticles are the value of current density and the form of current supply (changing polarity between electrodes and cyclic voltammetry), the concentration of reducible metal ions and their type (simple or complex), the nature and concentration of surfactant, temperature. With an increase in the current density, a decrease in the concentration of metal ions, and an increase in the concentration of surfactant, the size of MNPs is decreased, while with an increase in temperature, they are increased.

The use of the sacrificial anodes in combination with the changing of polarity between electrodes or cyclic voltammetry ensures the stability of the concentration of reducible metal ions, which contributes to the production of nanoparticles with a small dispersion in size.

In the scientific references, the electrochemical synthesis of nanoparticles of silver, gold, and platinum metals with the use of mainly synthetic polymer surfactants (PVP, PVA, PEG, NaPA) is mostly described. In recent years, there has been a tendency to use surfactants of natural origin (CHI, RL).

The absence of a reagent reducing agent in electrolytes and the use of non-toxic surfactants gives the reason to attribute the electrochemical synthesis of metal nanoparticles to "green" technologies. Electrochemical synthesis of metal nanoparticles in non-aqueous media – ionic liquids and organic aprotic solvents – is a promising direction. Electrolysis at cathodic potentials up to –3.0 V, the absence of the side cathodic processes and the indifference of such non-aqueous solutions to MNPs make it possible to increase their design possibilities and to expand the spectrum of nanoparticles due to metals for which $E^0_{Mn+/M} < 0$.

Funding

This work was carried out with the partial financial support of the National Research Foundation of Ukraine. Project registration number: 2020.02/0309 ("Design of polyfunctional nanostructured mono- and bimetals with electrocatalytic and antimicrobial properties").

Conflicts of Interest

The authors declare no conflict of interest.

References

1. Hochvaldová, L.; Večeřová, R.; Kolář, M.; Prucek, R.; Kvítek, L.; Lapčík, L.; Panáček, A. Antibacterial nanomaterials: Upcoming hope to overcome antibiotic resistance crisis. *Nanotechnol. Rev.* **2022**, *11*, 1115–1142, https://doi.org/10.1515/ntrev-2022-0059.
2. Anik, M.I.; Mahmud, N.; Masud, AA; Hasan, M. Gold nanoparticles (GNPs) in biomedical and clinical applications: A review. *Nano Select* **2022**, *3*, 792–828, https://doi.org/10.1002/nano.202100255.

3. Sztandera, K.; Gorzkiewicz, M.; Klajnert-Maculewicz, B. Gold Nanoparticles in Cancer Treatment. *Mol. Pharm.* **2019**, *16*, 1–23, https://doi.org/10.1021/acs.molpharmaceut.8b00810.
4. Jan, H.; Gul, R.; Andleeb, A.; Ullah, S.; Shah, M.; Khanum, M.; Ullah, I.; Hano, C.; Abbasi, B.H. A detailed review on biosynthesis of platinum nanoparticles (PtNPs), their potential antimicrobial and biomedical applications. *J. Saudi Chem. Soc*. **2021**, *25*, 101297, https://doi.org/10.1016/j.jscs.2021.101297.
5. Jabeen, S.; Qureshi, R.; Munazir, M.; Maqsood, M.; Munir, M.; Shah, S.S.H.; Rahim, B.Z. Application of green synthesized silver nanoparticles in cancer treatment – a critical review. *Mater. Res. Express* **2021**, *8*, 092001, https://doi.org/10.1088/2053-1591/ac1de3.
6. De Matteis, V.; Rizzello, L.; Cascione, M.; Liatsi-Douvitsa, E.; Apriceno, A.; Rinaldi, R. Green Plasmonic Nanoparticles and Bio-Inspired Stimuli-Responsive Vesicles in Cancer Therapy Application. *Nanomaterials* **2020**, *10*, 1083, https://doi.org/10.3390/nano10061083.
7. Ayipo, Y.O.; Bakare, A.A.; Badeggi, U.M.; Jimoh, A.A.; Lawal, A.; Mordi, M.N. Recent advances on therapeutic potentials of gold and silver nanobiomaterials for human viral diseases. *Curr. Res. Chem. Biol*. **2022**, *2*,100021, https://doi.org/10.1016/j.crchbi.2022.100021.
8. Zou, L.; Zhu, F.; Long, Z.-e.; Huang, Y. Bacterial extracellular electron transfer: a powerful route to the green biosynthesis of inorganic nanomaterials for multifunctional applications. *J. Nanobiotechnol*. **2021**, *19*, 120, https://doi.org/10.1186/s12951-021-00868-7.
9. Castillo-Henríquez, L.; Alfaro-Aguilar, K.; Ugalde-Álvarez, J.; Vega-Fernández, L.; de Oca-Vásquez, G.M.; Vega-Baudrit, J.R. Green Synthesis of Gold and Silver Nanoparticles from Plant Extracts and Their Possible Applications as Antimicrobial Agents in the Agricultural Area. *Nanomaterials* **2020**, *10*, 1763, https://doi.org/10.3390/nano10091763.
10. Salem, S.S.; Fouda, A. Green Synthesis of Metallic Nanoparticles and Their Prospective Biotechnological Applications: an Overview. *Biol. Trace. Elem. Res*. **2021**, *199*, 344–370, https://doi.org/10.1007/s12011-020-02138-3.
11. Shaheen, T.I.; El-Gamal, M.S.; Desouky, S.E.; Hassan, S.E.D.; Alemam, A.M. Benign Production of AgNPs/Bacterial Nanocellulose for Wound Healing Dress: Antioxidant, Cytotoxicity and In Vitro Studies. *J. Clust. Sci*. **2022**, *33*, 2735–2751, https://doi.org/10.1007/s10876-021-02190-6.
12. Jadoun, S.; Arif, R.; Jangid, N.K.; Meena, R.K. Green synthesis of nanoparticles using plant extracts: a review. *Environ. Chem. Lett*. **2021**, *19*, 355–374, https://doi.org/10.1007/s10311-020-01074-x.
13. Parmar, M.; Sanyal, M. Extensive study on plant mediated green synthesis of metal nanoparticles and their application for degradation of cationic and anionic dyes. *Environ. Nanotechnol. Monit. Manag*. **2022**, *17*, 100624, https://doi.org/10.1016/j.enmm.2021.100624.
14. Narasaiah, B.P.; Mandal, B.K. Remediation of azo-dyes based toxicity by agro-waste cotton boll peels mediated palladium nanoparticles. *J. Saudi Chem. Soc*. **2020**, *24*, 267–281, https://doi.org/10.1016/j.jscs.2019.11.003.
15. Sabela, M.; Balme, S.; Bechelany, M.; Janot, J.-M.; Bisetty, K. A Review of Gold and Silver Nanoparticle-Based Colorimetric Sensing Assays. *Adv. Eng. Mater*. **2017**, *19*, 1700270, https://doi.org/10.1002/adem.201700270.
16. Bigdeli, A.; Ghasemi, F.; Abbasi-Moayed, S.; Shahrajabian, M.; Fahimi-Kashani, N.; Jafarinejad, S.; Nejad, MAF; Hormozi-Nezhad, M.R. Ratiometric fluorescent nanoprobes for visual detection: Design principles and recent advances – A review. *Anal. Chim. Acta* **2019**, *1079*, 30–58, https://doi.org/10.1016/j.aca.2019.06.035.
17. Osonga, F.J.; Akgul, A.; Yazgan, I.; Akgul, A.; Eshun, G.B.; Sakhaee, L.; Sadik, O.A. Size and Shape-Dependent Antimicrobial Activities of Silver and Gold Nanoparticles: A Model Study as Potential Fungicides. *Molecules* **2020**, *25*, 2682, https://doi.org/10.3390/molecules25112682.
18. Rodrigues, T.S.; da Silva, A.G.M.; Camargo, P.H.C. Nanocatalysis by noble metal nanoparticles: controlled synthesis for the optimization and understanding of activities. *J. Mater. Chem. A* **2019**, *7*, 5857–5874, https://doi.org/10.1039/c9ta00074g.
19. Habibullah, G.; Viktorova, J.; Ruml, T. Current Strategies for Noble Metal Nanoparticle Synthesis. *Nanoscale Res. Lett*. **2021**, *16*, 47, https://doi.org/10.1186/s11671-021-03480-8.
20. Samanta, S.; Agarwal, S.; Nair, K.K.; Harris, R.A.; Swart, H. Biomolecular assisted synthesis and mechanism of silver and gold nanoparticles. *Mater. Res. Express* **2019**, *6*, 082009, https://doi.org/10.1088/2053-1591/ab296b.
21. Kapoor, R.T.; Salvadori, M.R.; Rafatullah, M.; Siddiqui, M.R.; Khan, M.A.; Alshareef, S.A. Exploration of Microbial Factories for Synthesis of Nanoparticles – A Sustainable Approach for Bioremediation of

Environmental Contaminants. *Front. Microbiol*. **2021**, *12*, 658294, https://doi.org/10.3389/fmicb.2021.658294.
22. Bahrulolum, H.; Nooraei, S.; Javanshir, N.; Tarrahimofrad, H.; Mirbagheri, V.S.; Easton, A.J.; Ahmadian, G. Green synthesis of metal nanoparticles using microorganisms and their application in the agrifood sector. *J. Nanobiotechnology* **2021**, *19*, 86, https://doi.org/10.1186/s12951-021-00834-3.
23. Mahmood Ansari, S.; Saquib, Q.; De Matteis, V.; Alwathnani, H.A.; Alharbi, S.A.; Al-Khedhairy, A.A. Marine Macroalgae Display Bioreductant Efficacy for Fabricating Metallic Nanoparticles: Intra/Extracellular Mechanism and Potential Biomedical Applications. *Bioinorg. Chem. Appl*. **2021**, *2021*, 5985377, https://doi.org/10.1155/2021/5985377.
24. Guilger-Casagrande, M.; de Lima, R. Synthesis of Silver Nanoparticles Mediated by Fungi: A Review. *Front. Bioeng. Biotechnol*. **2019**, *7*, 287, https://doi.org/10.3389/fbioe.2019.00287.
25. Izzi, M.; Sportelli, M.C.; Ditaranto, N.; Picca, R.A.; Innocenti, M.; Sabbatini, L.; Cioffi, N. Pros and Cons of Sacrificial Anode Electrolysis for the Preparation of Transition Metal Colloids: A Review. *ChemElectroChem*. **2020**, *7*, 386–394, https://doi.org/10.1002/celc.201901837.
26. Kuntyi, O.; Zozulya, G.; Kytsya, A. "Green" Synthesis of Metallic Nanoparticles by Sonoelectrochemical and Sonogalvanic Replacement Methods. *Bioinorg. Chem. Appl*. **2021**, *2021*, 9830644, https://doi.org/10.1155/2021/9830644.
27. Péter, L. Electrosynthesis of Nanostructures Without a Coating Formation on Electrodes. In Electrochemical Methods of Nanostructure Preparation. Monographs in Electrochemistry, Péter, L., Ed.; Springer, Cham, **2021**, 303–319, https://doi.org/10.1007/978-3-030-69117-2_9.
28. Katayama, Y. Electrochemical Preparation of Metal Nanoparticles in Ionic Liquids. In Nanocatalysis in Ionic Liquids, Prechtl, M.H.G., Ed.; Wiley-VCH Verlag GmbH & Co. KGaA, **2016**, 207–230, https://doi.org/10.1002/9783527693283.ch10.
29. Katayama, Y.; Oshino, Y.; Ichihashi, N.; Tachikawa, N.; Yoshii, K.; Toshima, K. Electrochemical preparation of palladium nanoparticles in bis (trifluoromethylsulfonyl)amide ionic liquids consisting of pyrrolidinium cations with different alkyl chain lengths. *Electrochim. Acta* **2015**, *183*, 37–41, https://doi.org/10.1016/j.electacta.2015.02.211.
30. Serizawa, N.; Kuwahara, S.; Katayama, Y. Electrochemical Behavior of Silver Halogenocomplexes in an Amide-Type Ionic Liquid. *J. Electrochem. Soc*. **2022**, *169*, 092502, https://doi.org/10.1149/1945-7111/ac8bac.
31. Sultana, S.; Tachikawa, N.; Yoshii, K.; Toshima, K.; Magagnin, L.; Katayama, Y. Electrochemical Preparation of Platinum Nanoparticles from Bis(acetylacetonato)platinum(II) in Some Aprotic Amide-type Ionic Liquids. *Electrochim. Acta* **2017**, *249*, 263–270, https://doi.org/10.1016/j.electacta.2017.08.021.
32. Sniekers, J.; Verguts, K.; Brooks, N.R.; Schaltin, S.; Phan, T.H.; Huynh, T.M.T.; Meervelt, L.V.; De Feyter, S.; Seo, J.W.; Fransaer, J.; Binnemans, K. Liquid Nickel Salts: Synthesis, Crystal Structure Determination, and Electrochemical Synthesis of Nickel Nanoparticles. *Chem. Eur. J*. **2016**, *22*, 1010–1020, https://doi.org/10.1002/chem.201504123.
33. Reetz, M.T.; Helbig, W. Size-Selective Synthesis of Nanostructured Transition Metal Clusters Clusters. *J. Am. Chem. Soc*. **1994**, *116*, 7401–7402, https://doi.org/10.1021/ja00095a051.
34. Reetz, M.T.; Helbig, W.; Quaiser, S.A.; Stimming, U.; Breuer, N.; Vogel, R. Visualization of Surfactants on Nanostructured Palladium Clusters by a Combination of STM and High-Resolution TEM. *Science* **1995**, *267*, 367–369, https://doi.org/10.1126/science.267.5196.367.
35. Rodríguez-Sánchez, L.; Blanco, M.C.; López-Quintela, M.A. Electrochemical Synthesis of Silver Nanoparticles. *J. Phys. Chem. B* **2000**, *104*, 9683–9688, https://doi.org/10.1021/jp001761r.
36. Vilar-Vidal, N.; Blanco, M.C.; Lopez-Quintela, M.A.; Rivas, J.; Serra, C. Electrochemical Synthesis of Very Stable Photoluminescent Copper Clusters. *J. Phys. Chem. C* **2010**, *114*, 15924–15930, https://doi.org/10.1021/jp911380s.
37. Chou, D.-W.; Huang, C.-J.; Liu, N.-H. Synthesis of the Small and Uniform Gold Nanoparticles by Electrochemical Technique. *J. Electrochem. Soc*. **2016**, *163*, D603, https://doi.org/10.1149/2.0491610jes.
38. Huang, C.-J.; Chiu, P.-H.; Wang, Y.-H.; Chen, K.-L.; Linn, J.-J.; Yang, C.-F. Electrochemically Controlling the Size of Gold Nanoparticles. *J. Electrochem. Soc*. **2006**, *153*, D193, https://doi.org/10.1149/1.2358103.
39. Yin, B.; Ma, H.; Wang, S.; Chen, S. Electrochemical Synthesis of Silver Nanoparticles under Protection of Poly(*N*-vinylpyrrolidone). *J. Phys. Chem. B* **2003**, *107*, 8898–8904, https://doi.org/10.1021/jp0349031.

40. Huang, S.; Ma, H.; Zhang, X.; Yong, F.; Feng, X.; Pan, W.; Wang, X.; Wang, Y.; Chen, S. Electrochemical Synthesis of Gold Nanocrystals and Their 1D and 2D Organization. *J. Phys. Chem. B* **2005**, *109*, 19823–19830, https://doi.org/10.1021/jp052863q.
41. Roldán, M.V.; Pellegri, N.; de Sanctis, O. Electrochemical Method for Ag-PEG Nanoparticles Synthesis. *J. Nanoparticles* **2013**, *2013*, 524150, http://doi.org/10.1155/2013/524150.
42. Surudzic, R.; Jovanović, Ž.; Bibić, N.; Nikolić, B.; Mišković-Stanković, V. Electrochemical synthesis of silver nanoparticles in poly(vinyl alcohol) solution. *J. Serb. Chem. Soc*. **2013**, *78*, 2087–2098, https://doi.org/10.2298/JSC131017124S.
43. Kuntyi, O.; Mazur, A.; Kytsya, A.; Karpenko, O.; Bazylyak, L.; Mertsalo, I.; Pokynbroda, T.; Prokopalo, A. Electrochemical synthesis of silver nanoparticles in solutions of rhamnolipid. *Micro Nano Lett*. **2020**, *15*, 802–807, https://doi.org/10.1049/mnl.2020.0195.
44. Nagaraju, DH; Lakshminarayanan, V. Electrochemical Synthesis of Thiol-Monolayer-Protected Clusters of Gold. *Langmuir* **2008**, *24*, 13855–13857, https://doi.org/10.1021/la803156a.
45. Fernandez-Blanco, C.; Heras, A.; Ruiz, V.; Colina, A. Spectroelectrochemical synthesis of gold nanoparticles using cyclic voltammetry in the presence of a protective agent. *RSC Adv*. **2014**, *4*, 45168–45173, https://doi.org/10.1039/c4ra07451c.
46. Pan, W.; Zhang, X.; Ma, H.; Zhang, J. Electrochemical Synthesis, Voltammetric Behavior, and Electrocatalytic Activity of Pd Nanoparticles. *J. Phys. Chem. C* **2008**, *112*, 2456–2461, https://doi.org/10.1021/jp710092z.
47. Uberman, P.M.; Pérez, L.A.; Martin, S.E.; Lacconi, G.I. Electrochemical synthesis of palladium nanoparticles in PVP solutions and their catalytic activity in Suzuki and Heck reactions in aqueous medium. *RSC Adv*. **2014**, *4*, 12330–12341, https://doi.org/10.1039/c3ra47854h.
48. Katayama, Y.; Endo, T.; Miura, T.; Toshima, K. Electrode Reactions of Platinum Bromide Complexes in an Amide-Type Ionic Liquid. *J. Electrochem. Soc*. **2013**, *160*, D423, http://doi.org/10.1149/2.008310jes.
49. Kuntyi, O.I.; Kytsya, A.R.; Mertsalo, I.P.; Mazur, A.S.; Zozula, G.I.; Bazylyak, L.I.; Topchak, R.V. Electrochemical synthesis of silver nanoparticles by reversible current in solutions of sodium polyacrylate. *Colloid Polym. Sci*. **2019**, *297*, 689–695, https://doi.org/10.1007/s00396-019-04488-4.
50. Hermanto, D.; Ismillayli, N.; Irmawanti, I.; Fathulloh, I.; Nila, D.; Zuryati, U.K.; Muliasari, H.; Wirawan, R. Electrochemically Synthesized Biogenic Silver Nanoparticles Using Green Tea Extract as a Promising Antioxidant. *Karbala Int. J. Mod. Sci*. **2023**, *9*, 8, https://doi.org/10.33640/2405-609X.3276.
51. McCann, K.; Cloud, JE; Yang, Y. Alternating voltage-induced electrochemical synthesis of colloidal Au nanoicosahedra. *J. Nanoparticle Res*. **2013**, *15*, 2065, https://doi.org/10.1007/s11051-013-2065-8.
52. Siddiqui, H.; Singh, N.; Khan, R.; Sharma, R.; Goswami, M.; Kumar, S.; Kumar, S.; Sathish, N.; Patel, S.S.; Khan, M.A.; Kumar, S. Sensitive SERS detection of *Tobramycin* using electrochemically synthesized silver nanoparticles. *Bull Mater. Sci*. **2022**, *45*, 211, https://doi.org/10.1007/s12034-022-02790-6.
53. Moshrefi, R.; Suryawanshi, A.; Stockmann, T.J. Electrochemically controlled Au nanoparticle nucleation at a micro liquid/liquid interface using ferrocene as reducing agent. *Electrochem. Commun*. **2021**, *122*, 106894, https://doi.org/10.1016/j.elecom.2020.106894.
54. Farshad, M.; Perera, D.C.; Rasaiah, J.C. Theoretical study of the stability, structure, and optical spectra of small silver clusters and their formation using density functional theory. *Phys. Chem. Chem. Phys*. **2021**, *23*, 25507–25517, https://doi.org/10.1039/d1cp04070g.
55. Simeonova, S.; Georgiev, P.; Exner, K.S.; Mihaylov, L.; Nihtianova, D.; Koynov, K.; Balashev, K. Kinetic study of gold nanoparticles synthesized in the presence of chitosan and citric acid. *Colloids Surf. A Physicochem. Eng. Asp*. **2018**, *557*, 106–115, https://doi.org/10.1016/j.colsurfa.2018.02.045.
56. Jagtap, N.R.; Shelke, V.A.; Nimase, M.S.; Jadhav, SM; Shankarwar, S.G.; Chondhekar, T.K. Electrochemical Synthesis of Tetra Alkyl Ammonium Salt Stabilized Gold Nanoparticles. *Synth. React. Inorg. Met. Org. Nano Met. Chem*. **2012**, *42*, 1369–1374, https://doi.org/10.1080/15533174.2012.680124.
57. Uberman, P.M.; Pérez, L.A.; Lacconi, G.I.; Martín, S.E. PVP-stabilized palladium nanoparticles electrochemically obtained as effective catalysts in aqueous medium Suzuki–Miyaura reaction. *J. Mol. Catal. A Chem*. **2012**, *363–364*, 245–253, https://doi.org/10.1016/j.molcata.2012.06.016.
58. Cha, J.-H.; Kim, K.-S.; Choi, S.; Yeon, S.-H.; Lee, H.; Lee, C.-S.; Shim, J.-J. Size-controlled electrochemical synthesis of palladium nanoparticles using morpholinium ionic liquid. *Korean J. Chem. Eng*. **2007**, *24*, 1089–1094, https://doi.org/10.1007/s11814-007-0126-3.

59. Cha, J.-H.; Park, S.-M.; Hong, Y.K.; Lee, H.; Kang, J.W.; Kim, K.-S. Electrochemical Preparation of Ionic Liquid-Stabilized Palladium Nanoparticles. *J. Nanosci. Nanotechnol*. **2012**, *12*, 3641–3645, https://doi.org/10.1166/jnn.2012.5590.
60. Kim, K.-S.; Kim, S.; Park, S.-M.; Kang, W.-K.; Kang, J.W. Size-selective Electrochemical Preparation of Alcohol Ionic-liquid-stabilized Palladium NPs. *J. Korean Phys. Soc*. **2010**, *57*, 1639–1643, https://doi.org/10.3938/jkps.57.1639.
61. Reetz, M.T.; Winter, M.; Breinbauer, R.; Thurn-Albrecht, T.; Vogel, W. Size-Selective Electrochemical Preparation of Surfactant-Stabilized Pd-, Ni- and Pt/Pd Colloids. *Chem. Eur. J*. **2001**, *7*, 1084-1094, https://doi.org/10.1002/1521-3765(20010302)7:5%3C1084::aid-chem1084%3E3.0.co;2-j.
62. Ledo-Suárez, A.; Rodríguez-Sánchez, L.; Blanco, M.C.; López-Quintela, M.A. Electrochemical synthesis and stabilization of cobalt nanoparticles. *Phys. Status Solidi (A)* **2006**, *203*, 1234–1240, https://doi.org/10.1002/pssa.200566196.
63. Jorge, G.A.; Martínez, J.D.; Bullón, M.C.; de Sousa, D.; de Navarro, C.U. Electrochemical Synthesis of Rhodium Nanoparticles and their Characterization by Transmission Electron Microscopy (TEM). *Portugaliae Electrochim. Acta* **2009**, *27*, 279–287, https://doi.org/10.4152/pea.200903279.
64. Sosa, M.; Bullón, M.C.; de Navarro, C.U.; Jorge, G.; Martínez, J.D. Estudio de nanopartículas bimetálicas de Rh-Pd sintetizadas por vía electroquímica. *ACI* **2011**, *2*, 89–99, https://doi.org/10.13140/2.1.4684.3525.
65. Jovanović, Ž.; Stojkovska, J.; Obradović, B.; Mišković-Stanković, V. Alginate hydrogel microbeads incorporated with Ag nanoparticles obtained by electrochemical method. *Mater. Chem. Phys*. **2012**, *133*, 182–189, https://doi.org/10.1016/j.matchemphys.2012.01.005.
66. Cioffi, N.; Colaianni, L.; Ieva, E.; Pilolli, R.; Ditaranto, N.; Angione, MD; Cotrone, S.; Buchholt, K.; Spetz, A.L.; Sabbatini, L.; Torsi, L. Electrosynthesis and characterization of gold nanoparticles for electronic capacitance sensing of pollutants. *Electrochim. Acta*. **2011**, *56*, 3713–3720, https://doi.org/10.1016/j.electacta.2010.12.105.
67. Tang, S.; Meng, X.; Lu, H.; Zhu, S. PVP-assisted sonoelectrochemical growth of silver nanostructures with various shapes. *Mater. Chem. Phys*. **2009**, *116*, 464–468, https://doi.org/10.1016/j.matchemphys.2009.04.004.
68. Scotti, L.; Angelini, G.; Gasbarri, C.; Bucciarelli, T. Uncoated negatively charged silver nanoparticles: speeding up the electrochemical synthesis. *Mater. Res. Express* **2017**, *4*, 105001, https://doi.org/10.1088/2053-1591/aa8c39.
69. Pompilio, A.; Geminiani, C.; Bosco, D.; Rana, R.; Aceto, A.; Bucciarelli, T.; Scotti, L.; Di Bonaventura, G. Electrochemically Synthesized Silver Nanoparticles Are Active Against Planktonic and Biofilm Cells of Pseudomonas aeruginosa and Other Cystic Fibrosis-Associated Bacterial Pathogens. *Front. Microbiol*. **2018**, *9*, 1349, https://doi.org/10.3389/fmicb.2018.01349.
70. Nešović, K.; Janković, A.; Radetić, T.; Perić-Grujić, A.; Vukašinović-Sekulić, M.; Kojić, V.; Rhee, K.Y.; Mišković-Stanković, V. Poly(vinyl alcohol)/chitosan hydrogels with electrochemically synthesized silver nanoparticles for wound dressing applications. *J. Electrochem. Sci. Eng*. **2020**, *10*, 185–198, http://doi.org/10.5599/jese.732.
71. Gasbarri, C.; Ronci, M.; Aceto, A.; Vasani, R.; Iezzi, G.; Florio, T.; Barbieri, F.; Angelini, G.; Scotti, L. Structure and Properties of Electrochemically Synthesized Silver Nanoparticles in Aqueous Solution by High-Resolution Techniques. *Molecules* **2021**, *26*, 5155, https://doi.org/10.3390/molecules26175155.
72. Yan, K.; Xu, F.; Wei, W.; Yang, C.; Wang, D.; Shi, X. Electrochemical synthesis of chitosan/silver nanoparticles multilayer hydrogel coating with pH-dependent controlled release capability and antibacterial property. *Colloids Surf. B: Biointerfaces* **2021**, *202*, 111711, https://doi.org/10.1016/j.colsurfb.2021.111711.
73. Cloud, JE; McCann, K.; Perera, K.A.P.; Yang, Y. A Simple Method for Producing Colloidal Palladium Nanocrystals: Alternating Voltage-Induced Electrochemical Synthesis. *Small* **2013**, *9*, 2532–2536, https://doi.org/10.1002/smll.201202470.
74. Cloud, JE; Yoder, T.S.; Harvey, N.K.; Snow, K.; Yang, Y. A simple and generic approach for synthesizing colloidal metal and metal oxide nanocrystals. *Nanoscale* **2013**, *5*, 7368–7378, https://doi.org/10.1039/c3nr02404k.
75. Rabinal, M.K.; Kalasad, M.N.; Praveenkumar, K.; Bharadi, V.R.; Bhikshavartimath, A.M. Electrochemical synthesis and optical properties of organically capped silver nanoparticles. *J. Alloys. Compd*. **2013**, *562*, 43–47, http://doi.org/10.1016/j.jallcom.2013.01.043.

76. Wadkar, M.M.; Chaudhari, V.R.; Haram, SK Synthesis and Characterization of Stable Organosols of Silver Nanoparticles by Electrochemical Dissolution of Silver in DMSO. *J. Phys. Chem. B* **2006**, *110*, 20889–20894, https://doi.org/10.1021/jp063422p.
77. Becker, J.A.; Schäfer, R.; Festag. R.; Ruland, W.; Wendorff, J.H.; Pebler, J.; Quaiser, S.A.; Helbig, W.; Reetz, M.T. Electrochemical growth of superparamagnetic cobalt clusters. *J. Chem. Phys*. **1995**, *103*, 2520-2527, https://doi.org/10.1063/1.469673.
78. Sarcina, L.; García-Manrique, P.; Gutiérrez, G.; Ditaranto, N.; Cioffi, N.; Matos, M.; Blanco-López, M.d.C. Cu Nanoparticle-Loaded Nanovesicles with Antibiofilm Properties. Part I: Synthesis of New Hybrid Nanostructures. *Nanomaterials* **2020**, *10*, 1542, https://doi.org/10.3390/nano10081542.
79. Xu, G.; Qiao, X.; Qiu, X.; Chen, J. Green Synthesis of Highly Pure Nano-Silver Sols—Electrolysis. *Rare Metal. Mat. Eng*. **2013**, *42*, 249–253, https://doi.org/10.1016/S1875-5372(13)60040-5.
80. Fox, C.M.; Yu, T.; Breslin, C.B. Electrochemical formation of silver nanoparticles and their catalytic activity immobilised in a hydrogel matrix. *Colloid Polym. Sci*. **2020**, *298*, 549–558, https://doi.org/10.1007/s00396-020-04624-5.
81. Sarhan, A. Synthesis, spectroscopic investigation and bactericidal effect of Poly (vinyl alcohol) (PVA) - iron nanoparticles (Fe NPs). *Egypt. J. Chem*. **2020**, *63*, 4659–4669, https://doi.org/10.21608/ejchem.2020.34685.2725.
82. Lo, N.-C.; Tang, Y.-H.; Kao, C.-L.; Sun, I.-W.; Chen, P.-Y. Electrochemical formation of palladium nanoparticles in a salicylate-based hydrophilic ionic liquid: The effect of additives on particle morphology and electrochemical behavior. *Electrochem. Commun*. **2016**, *62*, 60–63, https://doi.org/10.1016/j.elecom.2015.12.001.
83. Sultana, S.; Tachikawa, N.; Yoshii, K.; Magagnin, L.; Toshima, K.; Katayama, Y. Electrochemical Behavior of Bis(acetylacetonato)platinum(II) Complex in an Amide-Type Ionic Liquid. *J. Electrochem. Soc*. **2016**, *163*, D401, https://doi.org/10.1149/2.0581608jes.
84. Hu, M.Z.; Easterly, C.E. A novel thermal electrochemical synthesis method for production of stable colloids of "naked" metal (Ag) nanocrystals. *Mater. Sci. Eng. C* **2009**, *29*, 726–736, https://doi.org/10.1016/j.msec.2009.01.018.
85. Wahab, M.A.; Luming, L.; Matin, M.A.; Karim, M.R.; Aijaz, M.O.; Alharbi, H.F.; Abdala, A.; Haque, R. Silver Micro-Nanoparticle-Based Nanoarchitectures: Synthesis Routes, Biomedical Applications, and Mechanisms of Action. *Polymers* **2021**, *13*, 2870, https://doi.org/10.3390/polym13172870.
86. Naganthran, A.; Verasoundarapandian, G.; Khalid, F.E.; Masarudin, M.J.; Zulkharnain, A.; Nawawi, N.M.; Karim, M.; Abdullah, C.A.C.; Ahmad, S.A. Characterization and Biomedical Application of Silver Nanoparticles. *Materials* **2022**, *15*, 427, https://doi.org/10.3390/ma15020427.
87. Parmar, S.; Kaur, H.; Singh, J.; Matharu, AS; Ramakrishna, S.; Bechelany, M. Recent Advances in Green Synthesis of Ag NPs for Extenuating Antimicrobial Resistance. *Nanomaterials* **2022**, *12*, 1115, https://doi.org/10.3390/nano12071115.
88. Dobre, N.; Petică, A.; Buda, M.; Anicăi, L.; Vişan, TELECTROCHEMICAL SYNTHESIS OF SILVER NANOPARTICLES IN AQUEOUS ELECTROLYTES. *U.P.B. Sci. Bull.* **2014**, *76*, 127–136.
89. Khaydarov, R.A.; Khaydarov, R.R.; Gapurova, O.; Estrin, Y.; Scheper, T. Electrochemical method for the synthesis of silver nanoparticles. *J. Nanoparticle. Res*. **2009**, *11*, 1193–1200, https://doi.org/10.1007/s11051-008-9513-x.
90. Mertsalo, I.P.; Mazur, A.S.; Kuntyi, O.I.; Zozulya, H.I. Electrochemical Preparation of Silver Polyacrylate Solutions Intended for the Synthesis of Silver Nanoparticles. *Mater. Sci*. **2020**, *55*, 716–723, https://doi.org/10.1007/s11003-020-00363-8.
91. Thuc, DT; Huy, T.Q.; Hoang, L.H.; Tien, B.C.; Chung, P.V.; Thuy, N.T.; Le, A.-T. Green synthesis of colloidal silver nanoparticles through electrochemical method and their antibacterial activity. *Mater. Lett*. **2016**, *181*, 173–177, https://doi.org/10.1016/j.matlet.2016.06.008.
92. Reicha, F.M.; Sarhan, A.; Abdel-Hamid, M.I.; El-Sherbiny, I.M. Preparation of silver nanoparticles in the presence of chitosan by electrochemical method. *Carbohydr. Polym*. **2012**, *89*, 236–244, https://doi.org/10.1016/j.carbpol.2012.03.002.
93. Huang, R.-H.; Chao, W.-K.; Yu, R.-S.; Huang, R.-T.; Hsueh, K.-L.; Shieu, F.-S. Facile Synthesis of Silver Nanoparticles by Electrochemical Method in the Presence of Sodium Montmorillonite. *J. Electrochem. Soc*. **2012**, *159*, E122, https://doi.org/10.1149/2.037206jes.
94. Hoang, V.-T.; Dinh, N.X.; Pham, T.N.; Hoang, T.V.; Tuan, P.A.; Huy, T.Q.; Le, A.-T. Scalable Electrochemical Synthesis of Novel Biogenic Silver Nanoparticles and Its Application to High-Sensitive

Detection of 4-Nitrophenol in Aqueous System. *Adv. Polym. Technol*. **2021**, *2021*, 6646219, https://doi.org/10.1155/2021/6646219.
95. Jiang, L.; Santiago, I.; Foord, J. High-Yield Electrochemical Synthesis of Silver Nanoparticles at Enzyme-Modified Boron-Doped Diamond Electrodes. *Langmuir* **2020**, *36*, 6089–6094, https://doi.org/10.1021/acs.langmuir.0c00375.
96. Huang, Z.; Jiang, H.; Liu, P.; Sun, J.; Guo, D.; Shana, J.; Gu, N. Continuous synthesis of size-tunable silver nanoparticles by a green electrolysis method and multi-electrode design for high yield. *J. Mater. Chem. A* **2015**, *3*, 1925-1929, https://doi.org/10.1039/c4ta06782g.
97. Nešović, K.; Mišković-Stanković, V. A comprehensive review of the polymer-based hydrogels with electrochemically synthesized silver nanoparticles for wound dressing applications. *Polym. Eng. Sci*. **2020**, *60*, 1393–1419, https://doi.org/10.1002/pen.25410 .
98. Kuntyi, O.; Shepida, M.; Sozanskyi, M.; Sukhatskiy, Y.; Mazur, A.; Kytsya, A.; Bazylyak, L. Sonoelectrochemical Synthesis of Silver Nanoparticles in Sodium Polyacrylate Solution. *Biointerf. Res. Appl. Chem*. **2020**, *11*, 12202–12214, http://doi.org/10.33263/briac114.1220212214.
99. Shepida, M.; Kuntyi, O.; Sozanskyi, M.; Sukhatskiy, Y. Sonoelectrochemical Synthesis of Antibacterial Active Silver Nanoparticles in Rhamnolipid Solution. *Adv. Mater. Sci. Eng*. **2021**, *2021*, 7754523, https://doi.org/10.1155/2021/7754523.
100. Zozulya, G.; Kuntyi, O.; Mnykh, R.; Sozanskyi, M. Synthesis of Antibacterially ActiveSilver Nanoparticles by Galvanic Replacement on Magnesium in Solutions of Sodium Polyacrylate in an Ultrasound. *Chem. Chem. Technol*. **2021**, *15*, 493–499, https://doi.org/10.23939/chcht15.04.493.
101. Zozulya, G.; Kuntyi, O.; Mnykh, R.; Kytsya, A.; Bazylyak, L. Synthesis of silver nanoparticles by sonogalvanic replacement on aluminium powder in sodium polyacrylate solutions. *Ultrason. Sonochem*. **2022**, *84*, 105951, https://doi.org/10.1016/j.ultsonch.2022.105951.
102. Ovais, M.; Raza, A.; Naz, S.; Islam, N.U.; Khalil, A.T.; Ali, S.; Khan, M.A.; Shinwari, Z.K. Current state and prospects of the phytosynthesized colloidal gold nanoparticles and their applications in cancer theranostics. *Appl. Microbiol. Biotechnol*. **2017**, *101*, 3551–3565, https://doi.org/10.1007/s00253-017-8250-4.
103. Timoszyk, A.; Grochowalska, R. Mechanism and Antibacterial Activity of Gold Nanoparticles (AuNPs) Functionalized with Natural Compounds from Plants. *Pharmaceutics* **2022**, *14*, 2599, 2599, https://doi.org/10.3390/pharmaceutics14122599.
104. Ielo, I.; Rando, G.; Giacobello, F.; Sfameni, S.; Castellano, A.; Galletta, M.; Drommi, D.; Rosace, G.; Plutino, MR Synthesis, Chemical–Physical Characterization, and Biomedical Applications of Functional Gold Nanoparticles: A Review. *Molecules* **2021**, *26*, 5823, https://doi.org/10.3390/molecules26195823.
105. Saldan, I.; Dobrovetska, O.; Sus, L.; Makota, O.; Pereviznyk, O.; Kuntyi, O.; Reshetnyak, O. Electrochemical synthesis and properties of gold nanomaterials. *J. Solid. State Electrochem*. **2018**, *22*, 637−656, https://doi.org/10.1007/s10008-017-3835-5.
106. Sierra-Rosales, P.; Torres, R.; Sepúlveda, C.; Kogan, M.J.; Squella, J.A. Electrochemical Characterization and Electrocatalytic Application of Gold Nanoparticles Synthesized with Different Stabilizing Agents. *Electroanalysis* **2017**, *29*, 386-396, https://doi.org/10.1002/elan.201700633.
107. AlMashrea, B.A.; Abla, F.; Chehimi, M.M.; Workie, B.; Han, C.; Mohamed, A.A. Polyaniline coated gold-aryl nanoparticles: Electrochemical synthesis and efficiency in methylene blue dye removal. *Synth. Met*. **2020**, *269*, 116528, https://doi.org/10.1016/j.synthmet.2020.116528.
108. Dechen, P.; Somsook, E. Synthesis and Characterization of Gold Nanoparticles Synthesized in Gel and Paper by Electrolysis. *Key. Eng. Mater*. **2019**, *824*, 163−167, https://doi.org/10.4028/www.scientific.net/KEM.824.163.
109. Haro-González, P.G.; Ramírez-Rico, D.S.; Larios-Durán, E.R. Synthesis of Gold Nanoparticles in Aqueous Solutions by Electrochemical Reduction Using poly(ethylen glicol) as stabilizer. *Int. J. Electrochem. Sci*. **2019**, *14*, 9704−9710, https://doi.org/10.20964/2019.10.10.
110. Saucedo-Espinosa, M.A.; Breitfeld, M.; Dittrich, P.S. Continuous Electroformation of Gold Nanoparticles in Nanoliter Droplet Reactors. *Angew. Chem. Int. Ed*. **2023**, *62*, e202212459, https://doi.org/10.1002/anie.202212459.
111. Liu, X.-y.; Cui, C.-y.; Cheng, Y.-w.; Ma, H.-y.; Liu, D. Shape control technology during electrochemical synthesis of gold nanoparticles. *Int. J. Miner. Metall. Mater*. **2013**, *20*, 486−492, https://doi.org/10.1007/s12613-013-0755-y.

112. Nasretdinova, G.R.; Osin, Y.N.; Gubaidullin, A.T.; Yanilkin, V.V. Methylviologen Mediated Electrosynthesis of Palladium Nanoparticles Stabilized with CTAC. *J. Electrochem. Soc*. **2016**, *163*, G99, https://doi.org/10.1149/2.1021608jes.
113. Uberman, P.M; García, C.S; Rodríguez, J.R; Martín, S.E. PVP-Pd nanoparticles as efficient catalyst for nitroarene reduction under mild conditions in aqueous media. *Green Chem*. **2017**, *19*, 739−748, https://doi.org/10.1039/c6gc02710e.
114. Wegner, S.; Janiak, C. Metal Nanoparticles in Ionic Liquids. *Top. Curr. Chem*. **2017**, *375*, 65, https://doi.org/10.1007/s41061-017-0148-1.
115. Manojkumar, K.; Sivaramakrishna, A.; Vijayakrishna, K. A short review on stable metal nanoparticles using ionic liquids, supported ionic liquids, and poly(ionic liquids). *J. Nanoparticle. Res*. **2016**, *18*, 103, https://doi.org/10.1007/s11051-016-3409-y.
116. Verma, C.; Ebenso, E.E.; Quraishi, M.A. Transition metal nanoparticles in ionic liquids: Synthesis and stabilization. *J. Mol. Liq*. **2019**, *276*, 826−849, https://doi.org/10.1016/j.molliq.2018.12.063.
117. Ludwig, T.; Singh, A.R.; Nørskov, J.K. Non-aqueous Solvent Adsorption on Transition Metal Surfaces with Density Functional Theory: Interaction of *N*,*N*-Dimethylformamide (DMF), Tetrahydrofuran (THF), and Dimethyl Sulfoxide (DMSO) with Ag, Cu, Pt, Rh, and Re Surfaces. *J. Phys. Chem. C* **2021**, *125*, 21943−21957, https://doi.org/10.1021/acs.jpcc.1c05724.
118. Li, N.; Bai, X.; Zhang, S.; Gao, Y.; Zheng, L.; Zhang, J.; Ma, H. Synthesis of Silver Nanoparticles in Ionic Liquid by a Simple Effective Electrochemical Method. *J. Dispers. Sci. Technol*. **2008**, *29*, 1059–1061, https://doi.org/10.1080/01932690701815606.
119. Fukui, R.; Katayama, Y.; Miura, T. The Influence of Potential on Electrodeposition of Silver and Formation of Silver Nanoparticles in Some Ionic Liquids. *J. Electrochem. Soc*. **2011**, *158*, D567, https://doi.org/10.1149/1.3610202.
120. Sniekers, J.; Geysens, P.; Malaquías, J.C.; Hoogerstraete, T.V.; Meervelt, L.V.; Fransaer. J.; Binnemans, K. Cobalt(II) containing liquid metal salts for electrodeposition of cobalt and electrochemical nanoparticle formation. *Dalton Trans*. **2017**, *46*, 12845−12855, https://doi.org/10.1039/c7dt02604h.
121. Katayama, Y.; Fukui, R.; Miura, T. Electrochemical Preparation of Cobalt Nano-particles in an Ionic Liquid. *Electrochemistry* **2013**, *81*, 532–534, https://doi.org/10.5796/electrochemistry.81.532.
122. Zhu, Y.-L.; Katayama, Y.; Miura, T. Electrochemical Preparation of Nickel and Iron Nanoparticles in a Hydrophobic Ionic Liquid. *Electrochem. Solid-State Lett.* **2011**, *14*, D110, https://doi.org/10.1149/2.010112esl.
123. Ando, K.; Tachikawa, N.; Serizawa, N.; Katayama, Y. Electrochemical Behavior of a Ni Chlorocomplex in a Lewis Basic Ionic Liquid Containing Chloride Ion. *J. Electrochem. Soc*. **2020**, *167*, 062505, https://doi.org/10.1149/1945-7111/ab7f21.
124. Saha, S.; Taguchi, T.; Tachikawa, N.; Yoshii, K.; Katayama, Y. Electrochemical Behavior of Cadmium in 1-Butyl-1-methylpyrrolidinium Bis(trifluoromethylsulfonyl)amide Room-temperature Ionic Liquid. *Electrochim. Acta* **2015**, *183*, 42−48, http://doi.org/10.1016/j.electacta.2015.05.018.
125. Manjum, M.; Serizawa, N.; Ispas, A.; Bund, A.; Katayama, Y. Electrochemical Preparation of Cobalt-Samarium Nanoparticles in an Aprotic Ionic Liquid. *J. Electrochem. Soc*. **2020**, *167*, 042505, https://doi.org/10.1149/1945-7111/ab79a8.
126. González, BS; Blanco, M.C.; López-Quintela, M.A. Single step electrochemical synthesis of hydrophilic/hydrophobic Ag_5 and Ag_6 blue luminescent clusters. *Nanoscale* **2012**, *4*, 7632−7635, https://doi.org/10.1039/c2nr31994b.